Pergamon

Marine Pollution Bulletin Vol. 43, Nos. 7–12, pp. 154–163, 2001

Printed in Great Britain
0025-326X/01 $ - see front matter

PII: S0025-326X(01)00055-8

Operational Monitoring and Forecasting in the Aegean Sea: System Limitations and Forecasting Skill Evaluation

K. NITTIS*, V. ZERVAKIS, L. PERIVOLIOTIS, A. PAPADOPOULOS and G. CHRONIS
National Centre for Marine Research (NCMR), A. Kosmas Hellinikon, 16604 Athens, Greece

The POSEIDON system, based on a network of 11 oceanographic buoys and a system of atmospheric/oceanic models, provides real-time observations and forecasts of the marine environmental conditions in the Aegean Sea. The buoy network collects meteorological, sea state and upper-ocean physical and biochemical data. The efficiency and functionality of the various system components are being evaluated during the present pre-operational phase and discussed in this paper. The problem of bio-fouling on optical and chemical sensors is found to be a main limitation factor on the quality of data. Possible solutions to this problem as well as quality control methods that are being developed are also described. Finally, an evaluation of the numerical models is presented through the estimation of their forecasting skill for selected periods. © 2001 Elsevier Science Ltd. All rights reserved.

Keywords: mathematical models; data processing; currents; physical properties; operational oceanography; Aegean Sea.

Introduction

The goal of Operational Oceanography is to provide in real time reliable information and forecasts for marine environmental conditions, in order to support all kinds of activities in the sea. It is a relatively young branch of marine sciences that was developed during the past two decades aiming to fulfil the continuously increasing demands for sustainable exploration and exploitation of marine resources. Today, Operational Oceanography has been recognized by many international organizations (IOC, WMO, ICSU) as a high priority of marine scientific research (Flemming, 1995). This interest has been expressed by the foundation of the Global Ocean Observing System (GOOS), an initiative also supported by the Agenda 21 report published by the United Nations in 1992. The role of this organization is to promote and coordinate international and national efforts for the development of large-scale and regional ocean observing and forecasting systems (IOC, 1998).

The EuroGOOS (Woods *et al.*, 1996) initiative has coordinated during the past 6 years activities on ocean observation and forecasting and helped to advance operational oceanography on a European level. The EuroGOOS plan introduces six regional projects that, in their first phase, demonstrate the potential of collaboration between agencies in creating operational services, while in their final phase they establish operational forecasting systems in the regional seas of Europe. The Mediterranean Forecasting System (Pinardi and Flemming, 1998) is one of the regional test cases, which is already in the end of the first phase. During this phase, the possibility of basin scale weekly forecasts with assimilation of near real time data was demonstrated.

The TAO array of the Equatorial Pacific is probably the most important international effort for large-scale monitoring in the deep open ocean (McPhaden, 1995). Due to the tight-coupling between atmosphere and ocean in the tropics, the TAO array observations have increased the forecasting skill of sea surface temperature (SST) to more than 12 months. In the east coast of the United States, a pre-operational nowcast/forecast system focused on coastal area processes has been set up and evaluated during the past 5 years (Aikman *et al.*, 1996). The observational basis of the system was the remote sensing data (SST and Sea Surface Height – SSH) that were assimilated into the model forecasts. Finally, the SeaWatch-Europe was a multi-national effort to develop a monitoring and forecasting system for the marine environment in northern Europe (Hansen and Stel, 1997). Based on a network of oceanographic buoys, the system developed a number of applications related to pollution monitoring, weather forecasting, detection of algal blooms, etc.

*Corresponding author. Fax: +30-1-9946-162.
E-mail address: knittis@ncmr.gr (K. Nittis).

The POSEIDON project, presented in this paper, used many of the innovations of the SeaWatch project, in order to develop a state-of-the art system for the operational monitoring and forecasting of marine environmental conditions in the Aegean Sea (Soukissian *et al.*, 1999). It had a 36-months duration and was completed by the end of May 2000. In this paper we describe the various components of the POSEIDON system and we discuss their functionality and limitations. We also present a preliminary evaluation of the numerical forecasting components, which are in pre-operational use since January 2000.

System Configuration

The two main components of POSEIDON are the data collection – transmission system and the numerical forecasting component. Observations are based on a network (Fig. 1) of 11 SeaWatch oceanographic buoys manufactured by Oceanor. Each buoy is equipped with meteorological (wind speed and direction, air temperature, atmospheric pressure) and oceanographic parameters (waves, current speed and direction, temperature, salinity, dissolved oxygen, chlorophyll-α and radioactivity in two buoys). Temperature and salinity are measured at 5 depths between 3 and 50 m, while all other parameters are measured at 3 m depth. The type of sensors used is presented in Table 1. Sampling is carried out every 3 h and then data are automatically pre-processed on the buoy and transmitted to the operational center of NCMR via INMARSAT-C and GSM communications.

As soon as the data arrive to the operational center, an automatic routine check of battery level and station position is carried out, in order to detect possible energy problems or buoy drifting events. A first-level quality control detects values outside the predefined ranges of natural variability and checks for spikes and stationary values. Data are then inserted to the POSEIDON database and published to the Internet through the project's web page. A second-level quality check that detects slow trends due to sensor's drifting or bio-fouling is carried out every 2–3 months when buoy maintenance is carried out.

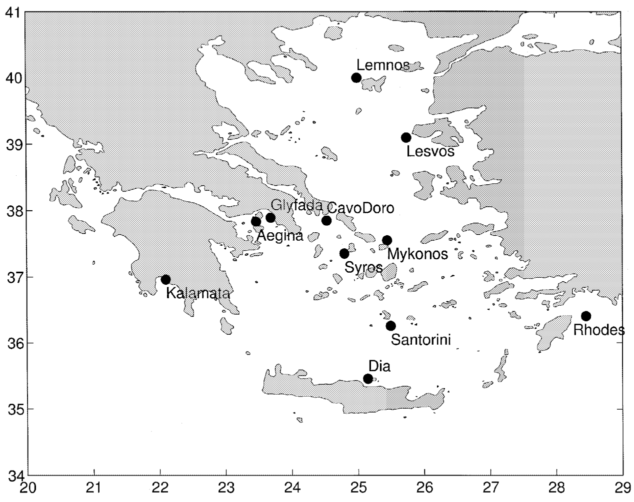

Fig. 1 The POSEIDON buoy network.

TABLE 1
Sensors available on SeaWatch buoys.

Parameter	Instrument – sensor type
Air temperature	Omega Engineering ON-905-44036
Atmospheric pressure	Vaisala PTB200
Wind speed – direction	Lambrecht 1453 S2 F1000
Waves	Seatex MRU-4
Current	NE Sensortec UCM-60
T,S at 3 m	NE Sensortec UCM-60, with Aanderaa 2990 inductive cell, Kistler Pressure sensor and CS4-1/10 Temperature sensor
T,S 0–50 m	Seamos CTD string equipped with Conductivity cell Aanderaa 2994, temperature sensor Fenwall GB 32JM19 and pressure sensor Keller, PA-10H/8634
Oxygen	Royce Instruments Model 94
Chlorophyll-a	Chelsea Instruments Mini Track Mark II fluorimeter
Radioactivity	Oceanor RADAM

The forecasting system is based on a hierarchy of numerical models that provide every day a 72 h forecast. The first one is the atmospheric model that provides meteorological forcing at the air–sea interface for the oceanographic models. The hydrodynamic model provides forecasts of three-dimensional current fields and hydrological characteristics while the offshore wave model is forecasting the wave spectrum and the derived parameters of interest i.e., wave height, period and direction. In the following paragraphs we present the characteristics of these three models with emphasis on the meteorological and hydrodynamic models for which a preliminary evaluation is carried out.

The weather forecasting system is based on the SKIRON model, developed at the University of Athens (Kallos *et al.*, 1997). Its central component is the Eta limited area model that was originally developed at the University of Belgrade (Janjic, 1994; Mesinger *et al.*, 1988). The system was configured to provide high-resolution weather forecasts over the Aegean Sea where the waves and hydrodynamic models are applied. It is developed to operate in fully automatic unattended mode under Unix operational system. In order to achieve the best possible temporal resolution in the area of interest, the system is applied in two different configurations. The first simulation is performed with coarser resolution (COARSE) and the second one with the high resolution (FINE). The COARSE version of the model has a resolution of 0.24 degree and covers the area 24.2°W to 51.8°E and 12.9°N to 53.4°N. In the vertical, 32 levels are used stretching from ground to the model top (15 800 m). For the initial and the boundary meteorological conditions the NCEP (National Centre for Environmental Prediction, USA) objective analysis grid data are used, in a 1.25°-resolution, for 10 standard pressure levels (1000, 850, 700, 500, 400, 300, 250, 200, 150 and 100 h Pa). The above data are downloaded daily from NCEP. The model updates its boundary conditions every 6 h. For SST, the NCEP 1-2-1 time filtered weekly data, at 1×1 degree resolution are used. The FINE version cover the area 2.6°E to 38.4°E and 27.4°N to 49.5°N, with horizontal resolution of 0.10°. The distribution of the vertical layers is the same as in the COARSE model. The meteorological fields, as they are produced by the COARSE model, provide the appropriate initial and boundary meteorological conditions for the FINE model. In this way, the simulation with the FINE model is performed utilizing 24 standard pressure levels and updates its boundary conditions every 1-h. For SST, the same grid data from NCEP are used. The main products of the system are precipitation, snowfall, cloud coverage, temperature at 2 m, wind speed at 10 m, surface pressure, fog, dust concentration and deposition, as well air temperature and wind speed at specific standard iso-pressure levels. Model results are processed and all the necessary input for the waves and the ocean hydrodynamic models are prepared automatically.

The hydrodynamic model developed by the University of Athens (Physical Oceanography Group) is based on the so-called Princeton Ocean Model (Blumberg and Mellor, 1987). It is a 3-D, primitive equation model that has been tested in both open sea and coastal areas. It has been applied in various regional studies in the Mediterranean Sea (Zavatarelli and Mellor, 1995; Zavatarelli and Pinardi, 1995; Nittis and Lascaratos, 1998), while it has been recently used for an operational forecasting system of the Mediterranean (Horton *et al.*, 1997). It is applied in the Aegean Sea with a high-resolution grid of 0.05° in the horizontal and 30 layers in the vertical. In this resolution the model is able to reproduce eddy dynamics that play a major role on the circulation field especially in the synoptic time scale. The prognostic variables are the sea level elevation, the three components of velocity, temperature, salinity, turbulent kinetic energy and turbulence macroscale. The last two parameters are part of the turbulence closure scheme that provides realistic parameterization of vertical mixing (Mellor and Yamada, 1982). Wind stress, heat and water fluxes provide the surface boundary forcing conditions. These fluxes are interactively computed by the model, using bulk formulas that combine the model's SST with the forecasted atmospheric variables (Lascaratos and Nittis, 1998). On the open boundaries, an upstream advection equation is used for salinity, temperature and the tangential component of velocity. When there is inflow through the open boundary, temperature and salinity are prescribed from the seasonal climatology. A free radiation and a Sommerfeld radiation condition are used for the normal to the boundary depth integrated and baroclinic velocities, respectively. Since June 2000, boundary values are provided by a 0.1°-resolution model of the whole Eastern Mediterranean that runs in parallel to the Aegean model with the same configuration.

The offshore waves model simulates the dynamics of wind-generated waves in the open sea with the horizontal resolution of 0.05°. The prognostic parameter is the wave spectrum and all the deriving operational quantities such as significant wave height, main wave direction and significant-mean wave periods (Christopoulos, 1997). The model is using the 72 h forecast of the atmospheric model and the currents field from the ocean hydrodynamic prediction model in order to incorporate currents induced refraction to the wave propagation. Data assimilation procedures (optimal interpolation scheme) have been tested but they are not used in the daily operational forecast.

System Limitations

A major challenge for marine operational monitoring systems is the data quality assurance. The oceanographic sensors used on buoys and other autonomous measuring devices (drifters etc.,) have different characteristics, and thus limitations, from those used for typical data sampling from R/V (CTDs and lab analysis). A major problem for the instruments and sensors that remain deployed for a long time, is the effect of bio-fouling. The problem is strongly dependent on the biochemical characteristics of the area and the measuring method used by the sensors. In oligotrophic areas with low levels of phytoplankton the problem is much smaller than in areas with relatively eutrophic conditions. Furthermore, sensors that use optical measurements (e.g., measurement of chl-α or turbidity) are much more sensitive to bio-fouling.

A second factor that controls the maintenance-free period of a sensor is the need for fresh spare parts or consumables. The sensor of oxygen that needs new membrane and electrolyte every approximately 2–3 months is a characteristics example. In Fig. 2 we present

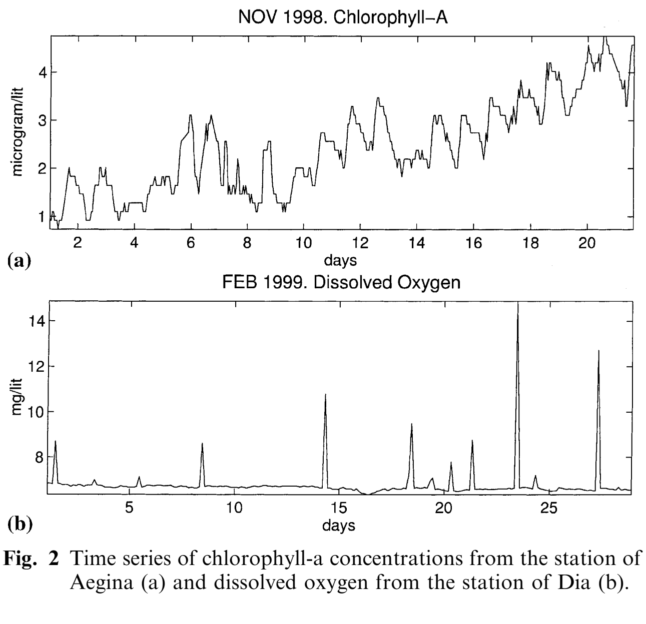

Fig. 2 Time series of chlorophyll-a concentrations from the station of Aegina (a) and dissolved oxygen from the station of Dia (b).

examples of sensors malfunction due to the above problems. The spikes observed in the time-series of dissolved oxygen are 2.5 months after the maintenance of the specific buoy in the Cretan Sea (Dia station). The increasing trend in the chl-α time series is a characteristic example of bio-fouling effect. It was observed approximately 40 days after the deployment of the buoy in the Saronikos gulf (Aegina station), an area with relatively high concentrations of phytoplankton. The typical maintenance-free period for the various sites in the Aegean Sea was estimated to approximately 2–3 months.

Apart from the above limiting factors that control the quality of the real-time data, the frequent calibration of the sensors, especially for those that are sensitive to bio-fouling, is a procedure that was found to be necessary in frequent time intervals. A main reason for re-calibration of sensors is the fact that some of them are designed and calibrated for a range of values different from the physical variability in the area of interest. A characteristic example is the sensor of chl-α that works in a range of 0–75 μg l^{-1}, while the variability is the Aegean Sea is 0.1–1 μg l^{-1} with maximum values up to 10 μg l^{-1} during spring blooms. For this reason, a calibration procedure is carried out on board the R/V Aegaeo during each maintenance cruise. The calibration is performed on the most sensitive to bio-fouling sensors, i.e., the sensors of conductivity, chl-α fluorescence (chl-α) and dissolved oxygen (DO) concentration. The calibration procedure has been planned in such a way as to minimize ship-time demands and cover the widest possible range for each parameter.

In order to satisfy the first requirement, the sampling interval of each SeaWatch buoy (once retrieved and undergone the regular maintenance procedure) is set at 15 min: of the above, 10 min are left between measurements, allowing time to change water samples to-be-measured, and 5 min are reserved for the actual measurement. Thus, for 6–8 samples necessary to define a calibration curve, a ship-time of 1.5–2 h is reserved for calibration of each buoy. This time is usually spent steaming between the old and the new position of the buoy that's being calibrated. Once the measurements are finished, the sampling interval is set back to 3 h, and the buoy is ready for deployment in its new position.

In order to cover as large a range of values as possible for each parameter, a different experiment had to be devised for conductivity, chl-α and DO. For the conductivity calibration, a thermally insulated, 1 m^3 calibration tank has been built. The highest conductivity values are achieved by filling the tank with local, highly saline surface water (and occasionally, warming it). Lower conductivity values are achieved by adding fresh water from the ship between measurements. A Seabird SBE-19 CTD provides conductivity measurements for reference values. To achieve a high range of values of DO, a large stock of water is obtained from the deep waters of the near-anoxic Epidaurus bay, at the beginning of each maintenance cruise. The range of values is achieved by various mixtures of the low DO stock water with highly oxygenated surface water from each site. The industry-standard Winkler method (Carpenter, 1965a,b) provides reference values for each measurement. The wide range of values in the chl-α domain is provided by the high variability of chl-α within the upper 100 m of the water column at each site. Reference values are obtained through the use of a high-accuracy fluorometer TURNER 00-AU-10 fluorometer in the ship's lab. The fluorescence values are converted to phytoplankton concentration using the formula of Yentsch and Menzel (1963).

In general, the ship borne calibration has been able to confirm the quality of conductivity (Fig. 3) and dissolved oxygen measurements, and significantly improves the quality of chl-α measurements. Concerning conductivity, poor mixing in the calibration tank has not yet enabled us to significantly improve the factory calibration, however better mixing equipment is under construction. Dissolved oxygen sensors function very satisfactorily, and the in situ calibration has only been able to provide small corrections of temperature-related trends (Owens and Millard, 1985). The fluorescence calibration has resulted in greatly improving the measurements, which were of very poor quality using factory coefficients, probably due to the oligotrophic nature of the Aegean marine environment.

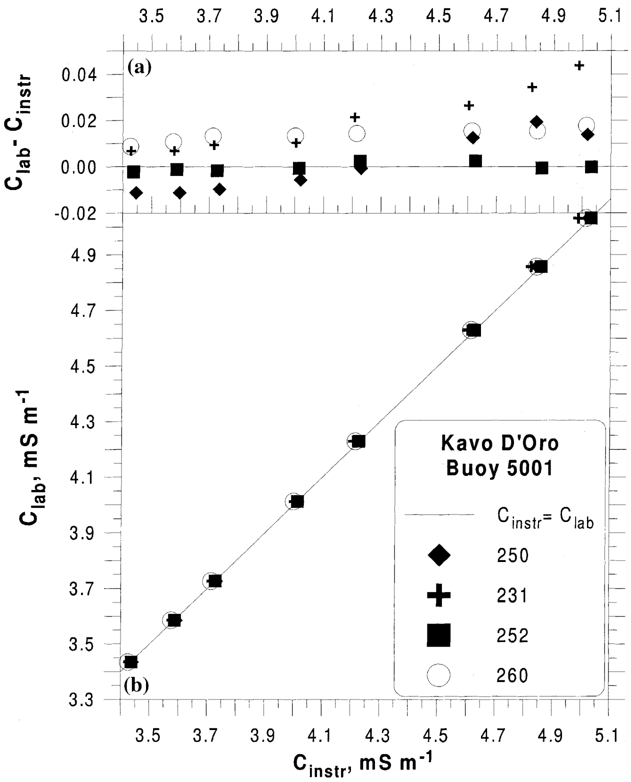

Fig. 3 Conductivity calibration resume plot for buoy 5001: reference (SBE-19 CTD) conductivity (b) and sensor – reference difference (a) are plotted versus the conductivity of each sensor of the C/T string. The figure shows data from the four sensors (250, 231, 252 and 260) comprising the C/T string. Note that most measurements fall within 0.2 ms m^{-1} from reference measurements.

Selected System Applications

The POSEIDON network data are used for a wide range of applications, such as safety of navigation and operations in the sea, monitoring of pollution, etc. In the same time, they compose a unique data set for various research studies, such as air–sea interaction mechanisms, wave generation processes, physical-biological coupling, etc. In the following paragraphs we present two examples that demonstrate the value of the POSEIDON data for such studies.

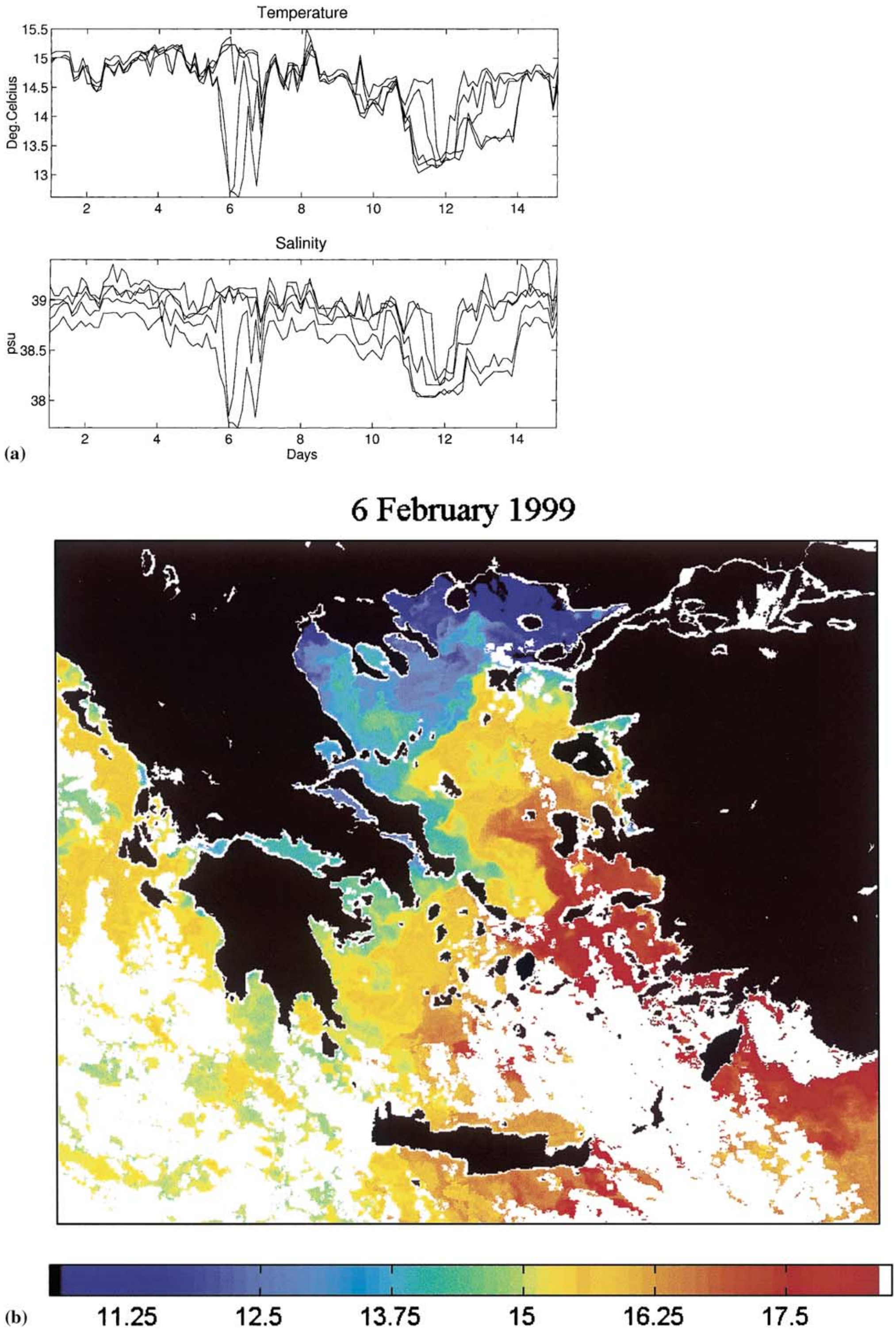

Fig. 4 (a) Time series of temperature and salinity at various depths (3–45 m) at Lemnos station for the period 1–15 February 1999, (b) Sea surface temperature map derived from NOAA AVHRR image of 6 February 1999.

In Fig. 4(a) we present time series of temperature and salinity from a station located NW of Lemnos island in the north Aegean Sea. The period presented is 1–15 February 1999 and the different lines correspond to depths from 3 to 45 m. During the first 6 days of the month, the upper 50 m appear to be well mixed with temperature of 14.5–15°C and salinity of 38.7–39.2 psu. During the next days the buoy recorded two pulses of abrupt temperature and salinity decrease. The first event had 1day duration and affected the upper 10 m where the temperature drop was more than 2°C and the salinity drop more than 1 psu. The second event affected the upper 20 m for more than 3 days (11–14 February) while the signal reached the lower layers only for few hours during 12 February. The corresponding temperature and salinity drop was 1.5°C and 8 psu, respectively. Both events are attributed to advection of fresh and cold waters of Black Sea origin that outflow from the Dardanelle's straits. These waters can be clearly observed in the SST map derived from the AVHRR image of 6 February (Fig. 4(b)). A strong temperature front is observed to the north of the Lemnos Island. The observed pulses are associated either to the instability of this front or to advection of cold patches that detach from the main pool of Black Sea water that seem to be confined during that period in the NE corner of the basin. Apart of their distinct temperature and salinity characteristics, these waters can also be traced by their increased nutrients and chl-α concentrations. Indeed the Black Sea is a eutrophic area due to the discharge of high amounts of nutrients by the major European rivers that outflow in the basin. These rivers are, in the same time, a potential source of pollution for the Black Sea and consequently for the Aegean. Therefore, the continuous monitoring of the Dardanelle's outflow through the POSEIDON network is a significant contribution to the protection of the marine environment in the Aegean Sea.

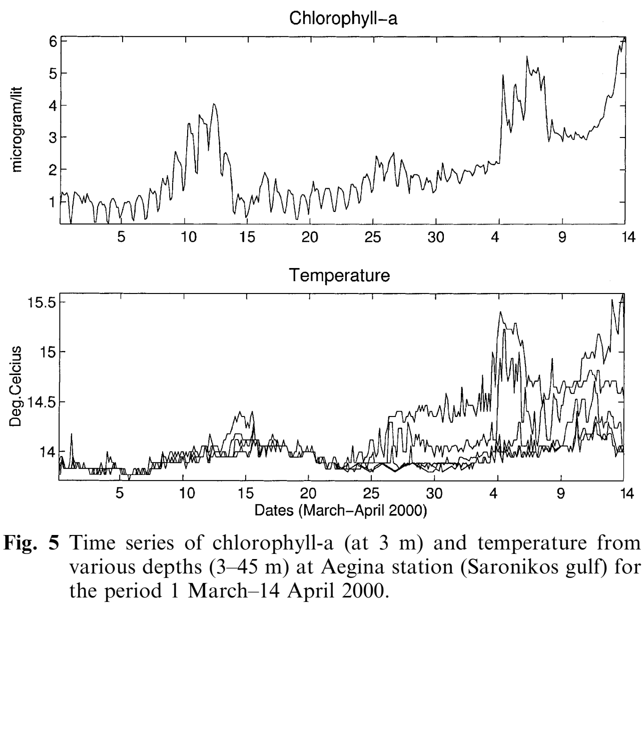

Fig. 5 Time series of chlorophyll-a (at 3 m) and temperature from various depths (3–45 m) at Aegina station (Saronikos gulf) for the period 1 March–14 April 2000.

The second example is from the station of Aegina in the Saronikos Gulf. In Fig. 5 we present time series of chl-α concentrations (at 3 m depth) and temperature (at the 3–45 m layer) for the period 1 March–14 April 2000. The variations of chl-α concentrations are related to the increase of phytoplankton during the spring, a phenomenon also known as 'spring bloom'. At least three events of temporary increase of phytoplankton concentrations can be observed on the 11the and 27th March and 7th April. Before this series of events chl-α concentrations retain the relatively low values below 1 μg l^{-1} that characterize the oligotrophic Aegean Sea, while during the events maximum values up to 6 μg l^{-1} were recorded. This variability of chl-α concentrations appears to be correlated to variations of temperature. Theoretically, the generation of the seasonal thermocline that traps the nutrients in the euphotic zone is the main reason for the increased primary production that leads to the spring bloom (Sverdrup, 1953). This seems to be the case at least for the events of 27th of March and 5th of April. The first event of 11 March does not seem to be clearly related to this mechanism since the vertical stratification starts on the 14th when the phytoplankton concentration starts to decrease again. The above example shows that the POSEIDON network can be used for the detection of eutrophication mechanisms and for studies on physical – biological coupling.

Evaluation of Models Forecasting Skill

The POSEIDON numerical forecasting system is in preoperational use since September 1999. Since that time, all three numerical models run daily giving 72-h forecasts. These forecasts are being evaluated continuously through direct comparison to buoy data or independent sources of information such as satellite maps (for SST) or data from land based meteorological stations. Based on these comparisons, various model components were tested and developed in order to improve forecasts. Results from this evaluation procedure for the meteorological model as well as preliminary results for the hydrodynamic model are presented in this section; similar results for the wave model have been presented by Christopoulos *et al.* (2000). The calculations presented below are for the period 1/3/2000 to 17/5/2000 using the point measurements of the POSEIDON buoy network and the first 24 h model forecasts.

In order to compare observations and forecasted fields at the various locations, the atmospheric model results were interpolated to each observation site using an inverse distance method (Cressman, 1959)

$$M = \frac{\sum_{i=1}^{4} w_i \cdot M_i}{\sum_{i=1}^{4} w_i},$$

where M_i is the model values at the four model grid points surrounding the observation. The weight w_i given to the surrounding values is specified from

$w_i = 1/r_i^2$,

where r_i is the distance from i model grid point to the observation.

Even if measurements are accurate at their location, the observations are essentially point measurements and may not be representative of an area mean. According to this, the interpolated model values depend on the characterization of the surrounding four grid points as land or sea point. All buoy positions are close to the coast so the corresponding surrounding four model grid points include land points. This means that interpolated model wind speed may be weaker and interpolated model air temperature may follow the diurnal variation of temperature over land.

Three basic statistical measures mean error (BIAS), the percentage bias score (B_{score}) and the root mean square error (RMSE) were used to assess forecast performance. There are given by (Wilks, 1995)

$$\text{BIAS} = \frac{1}{N} \cdot \sum_{i=1}^{N} (M_i - O_i) = \bar{M} - \bar{O},$$

$$\text{RMSE} = \sqrt{\frac{\sum_{i=1}^{N} (M_i - O_i)^2}{N}},$$

$$\text{BIAS}_{\text{score}} = 100 \cdot \frac{1}{N} \cdot \sum_{i=1}^{N} \frac{M_i}{O_i},$$

where M_i is the model value at an observation point, O_i is the observed value and N the total number of the available observations at the specific location. In order to verify the model predictability for the wind direction, a threshold skill score is used. This skill score is based on a predefinition of a range of directions for which it is permitted for the model to decline. The skill score is given by: $Dir\ skill = 100 \times (S/N)$, where S is the number of correct predictions for the wind direction and N is the total number of observations at that location. A prediction is assumed a correct one when the model wind direction is between the range

$$M_i = O_i \pm R,$$

where M_i the model wind direction, O_i the observed wind direction and R the degrees that define the permissible range. The statistical results for the period 1/3/2000 to 17/5/2000 are shown in Tables 2–5.

The mean sea level pressure statistics

Both model configurations overestimate air pressure more than 1 hPa. Thoroughly, the BIAS for the

TABLE 2

The mean sea level pressure statistics.

	BIAS (mbar)		RMSE (mbar)		$\text{BIAS}_{\text{score}}$(%)	
	Coarse	Fine	Coarse	Fine	Coarse	Fine
Dia (Crete)	0.38	0.70	1.21	1.39	100.04	100.07
Aegina	0.02	0.38	1.10	1.29	100.00	100.04
Glyfada	0.15	0.48	1.22	1.40	100.02	100.05
Lesvos	0.35	0.73	1.13	1.45	100.03	100.07
Mykonos	0.51	0.84	1.29	1.52	100.05	100.08
Rhodes	0.81	1.24	1.42	1.83	100.08	100.12
Santorini	0.57	0.86	1.31	1.51	100.06	100.08
Kalamata	0.36	0.50	1.34	1.38	100.04	100.05
Syros	0.36	0.66	1.21	1.40	100.04	100.07
Cavo Doro	0.37	0.68	1.10	1.25	100.04	100.07
Total	0.40	0.72	1.25	1.46	100.04	100.07

TABLE 3

The air temperature statistics.

	BIAS (°C)		RMSE (°C)		$\text{BIAS}_{\text{score}}$(%)	
	Coarse	Fine	Coarse	Fine	Coarse	Fine
Dia (Crete)	−0.62	0.25	3.31	1.96	94.44	101.25
Aegina	−0.46	−0.01	2.73	2.00	95.51	99.80
Glyfada	−0.58	−0.19	3.38	3.25	92.82	96.60
Lesvos	−0.21	0.26	3.65	1.82	95.03	101.18
Mykonos	−1.28	−3.29	1.81	4.16	91.25	76.15
Rhodes	0.05	−0.36	3.37	3.18	98.25	95.92
Santorini	0.10	0.16	1.45	1.67	100.40	100.44
Kalamata	−1.20	−0.61	4.42	4.22	88.51	92.73
Syros	0.17	0.46	1.47	1.75	101.04	102.57
Cavo Doro	0.88	1.37	1.91	2.28	105.05	107.83
Total	−0.28	0.05	3.08	2.61	96.26	99.17

TABLE 4

The wind speed statistics.

	BIAS (m s^{-1})		RMSE (m s^{-1})		$\text{BIAS}_{\text{score}}$(%)	
	Coarse	Fine	Coarse	Fine	Coarse	Fine
Dia (Crete)	−1.24	−1.35	2.57	2.82	90.93	89.98
Aegina	−1.46	−2.46	2.54	3.45	84.18	71.07
Glyfada	−1.94	−3.02	3.03	3.86	77.54	62.75
Lesvos	−1.51	−1.60	2.65	2.67	85.46	84.65
Mykonos	−1.29	−2.07	3.01	4.04	91.17	83.36
Rhodes	−2.27	−1.47	3.24	2.57	73.36	85.03
Santorini	−0.44	−0.39	2.21	2.25	103.63	104.67
Kalamata	−1.28	−2.92	2.40	3.50	84.34	57.20
Syros	−0.27	−0.94	2.47	2.62	106.98	97.06
Cavo Doro	−1.97	−3.08	3.92	4.83	90.84	78.63
Total	−1.27	−1.45	2.71	2.87	89.75	87.88

TABLE 5

The wind direction statistics (% of success).

	$R = 22.5°$		$R = 45°$	
	Coarse	Fine	Coarse	Fine
Dia (Crete)	79.68	77.03	91.42	92.34
Aegina	80.00	74.28	83.73	83.99
Glyfada	78.79	82.46	89.39	92.54
Lesvos	83.79	82.55	94.66	93.53
Mykonos	75.61	60.98	78.05	68.29
Rhodes	78.56	79.67	91.87	91.50
Santorini	86.68	87.08	96.44	95.51
Kalamata	59.01	63.68	68.02	80.72
Syros	85.31	83.60	95.10	93.53
Cavo Doro	76.62	45.34	88.96	80.75
Total	79.06	77.33	89.12	90.00

COARSE model configuration ranges from 0.02 hPa to 0.81 hPa and RMSE ranges from 1.10 to 1.42 hPa, with a $BIAS_{score}$ almost equals 100%. Accordingly, the BIAS for the FINE model configuration ranges from 0.38 to 1.24 hPa and RMSE ranges from 1.25 to 1.83 hPa, with a $BIAS_{score}$ almost equals 100% (Table 2).

The air temperature statistics

There is a noticeable improvement in BIAS, RMSE and $BIAS_{score}$ when the horizontal resolution is decreased from 0.24° to 0.10° (Table 3). The FINE bias scores rise to around 99.17% from 96.26% of the COARSE bias scores. This can be explained by the fact that using the higher resolution increases the possibility to utilize model values from more sea-surrounding grid points than in case of the coarser resolution model. The use of higher resolution aids the diurnal variation of air temperature over land to influence less the interpolated model value at the observation location.

The wind statistics

The benefits of the use of the higher resolution are not recognizable when wind speed is examined. According to statistics (Table 4) COARSE seems to underestimate wind speed about 1.27 m s^{-1} and FINE about 1.45 m s^{-1} with a magnitude of errors up to 2.71 m s^{-1} for COARSE and 2.87 m s^{-1} for FINE. The percentage difference between observations and COARSE model values is almost 89.75% and between observations and FINE model values is almost 87.88%. The forecasting of wind direction is similar to both model configurations (Table 5). When the model wind directions are permitted to decline from observations up to 22.5° skill scores for both models are close to 80%. When the permissible declination is 45° the skill scores rises up to 90%.

Current and SST statistics

The above statistics were also calculated for the hydrodynamic model, for current speed and water temperature at the offshore stations of Lesvos, Mykonos, Santorini and Dia. The results (Table 6) indicate a high forecasting skill in SST (bias 0.1–0.8°C, score 99.8–104.7%) but a relative lower forecasting skill for the current (bias 2.3–7.1 cm s^{-1}, bias_score 74.5–135.7%). SST seems to be overestimated in Lesvos and Mykonos and slightly (0.1°C) underestimated in Santorini, with error around 1.0°C in all cases. Current speed is overestimated in almost all stations apart of Mykonos and the error is around 10 cm s^{-1} in all cases. We must note at this point that the extracted data from the model forecasts are not computed at the exact depth of the sensors (3 m) but at the surface layer of the model. Since this layer is usually much less that 3 m there is a systematic error introduced especially during the period that the surface thermocline develops. This mechanism is responsible for part of the bias since it tends to overestimate both temperature and current speed. The same statistics were also computed for the two components of the current speed (north-south and east-west). Time series of these components from the station of Lesvos are presented in Fig. 6. These computations show that the error is smaller in the alongshore component of the current. This is rather expected since all stations are very close to the coast and the model is less effective in computing the across-coast component in 1–2 grid-points off the coast. In the example of Lesvos station (Fig. 6) we can detect the two main frequencies that are common in all stations, one in the synoptic time scale (3–15 days) and one in the inertial period (19–21 h). In the alongshore component (NS) the model is able to follow the synoptic variability with overestimation of inertial waves during certain periods. In the across shore component (EW) there is a significant mismatch between model forecasts and observations in the synoptic variability.

TABLE 6

Current and water temperature statistics.

	BIAS		RMSE		$BIAS_{score}$	
	Current speed (cm s^{-1})	Temperature (°C)	Current speed (cm s^{-1})	Temperature (°C)	Current speed (%)	Temperature (%)
Lesvos	2.3	0.4	9.8	1.1	93.3	102.4
Mykonos	−6.0	0.8	10.7	1.0	93.4	104.7
Santorini	7.1	−0.1	9.9	0.8	135.7	99.8
Dia (Crete)	3.5	N/A	11.6	N/A	74.5	N/A

Summary and Concluding Remarks

The POSEIDON project has established an integrated marine environmental monitoring and forecasting system. The system uses the latest advancements of operational oceanography in both fields of sensors

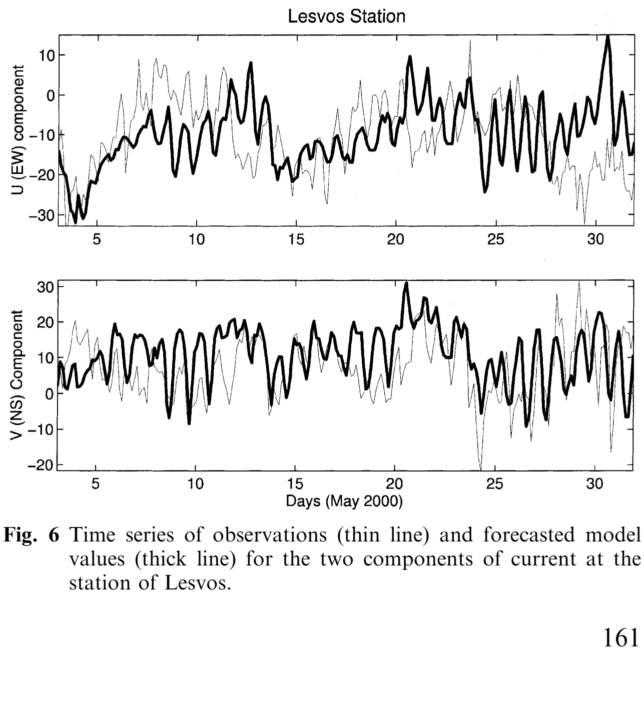

Fig. 6 Time series of observations (thin line) and forecasted model values (thick line) for the two components of current at the station of Lesvos.

technology and numerical modelling. In this paper we have described the functioning of the system and presented possible limitations related to autonomy (maintenance free period) and quality of data and forecasts. We also presented selected applications that show the capacity of the network data to extend our understanding of biological-physical processes (such as the spring bloom) and air–sea coupling on short and synoptic time scales.

Most of the oceanographic sensors that equip the buoys have a limited period of continuous operation in water without problems. The optical sensors are the most sensitive to bio-fouling that can create artificial trends on the resulting time series. A frequent (every 2–3 months) maintenance schedule, including re-calibration of sensors, was found to be able to guarantee the quality of data. The re-calibration procedure that has been adopted in the POSEIDON project is applied on conductivity, dissolved oxygen and chl-α sensors. This procedure is also used to adjust the transfer function of the sensor, usually calculated for a wide range of values, to the range of natural variability in the Aegean Sea.

A preliminary evaluation of the meteorological and hydrodynamic model's forecasting skill was also presented, based on statistical comparison between 24 h forecasts and in situ data from the buoy network. Despite the small period of evaluation, some preliminary remarks can be made. The atmospheric model has a remarkable forecasting skill for atmospheric pressure and air temperature, especially in the high resolution version, while the skill is lower for the wind field but still in very high levels (88–90%). The hydrodynamic model also presents high skill for SST but the current field forecasts are in some cases overestimated for more than 130%.

In the present configuration of the system, assimilation of buoy data is only used for the wave model. The experience of this application shows that in certain areas, the assimilation procedure may introduce large errors. Due to the complex topography of the Aegean Sea the spatial de-correlation scales are very low and the field cannot be considered, in most cases, isotropic. This problem is more pronounced in the case of currents, temperature and salinity fields that have even smaller temporal scales of variability. An additional limitation of the available buoy data is that they come from the upper 50 m and cannot, therefore, constrain the deeper flow. Despite these limitations, the development of assimilation schemes for current and hydrological data into the hydrodynamic model is underway and is expected to improve the model's forecasting skill. A parallel effort is the downscaling of the forecasting system to coastal areas with increased environmental problems and the development of ecological models for these areas.

The POSEIDON system has set the basis for operational forecasting in the Aegean Sea. It has already started to provide operational (data) and pre-operational (forecasts) services to the public and the whole effort can be considered a major contribution to the EuroGOOS. The future plans of the project include integration of additional data sources (e.g., satellite SST and SSH) and development of new numerical modules that will increase the model's forecasting skill and will extend the range of simulated processes and related system applications (pollution, biochemical cycles, etc.).

The POSEIDON project was funded by the Financial Mechanism of the European Economic Area – EFTA (85%) and the Hellenic Ministry of National Economy (15%).

Aikman, F., Mellor, G. L., Ezer, T., Sheinin, T., Chen, P., Breaker, L., Bosley, K. and Rao, D. B. (1996) Towards an operational nowcast/forecast system of the US East Coast. In *Modern Approaches to Data Assimilation in Ocean Modelling*, ed. P. Malanotte-Rizzoli, pp. 347–376. Elsevier Oceanography Series, 61.

Blumberg, A. F. and Mellor, G. L. (1987) A description of a three-dimensional coastal ocean circulation model. In *Three-Dimensional Coastal Ocean Circulation Models, Coastal Estuarine Science*, vol. 4, pp. 1–16. AGU, Washington DC.

Carpenter, J. H. (1965a) The accuracy of the Winkler method for the dissolved oxygen analysis. *Limnology and Oceanology* **10**, 135–140.

Carpenter, J. H. (1965b) The Chesapeake Bay Institute technique for dissolved oxygen method. *Limnology and Oceanology* **10**, 141–143.

Christopoulos, S. (1997) Wind wave modelling aspects within complicated topography. *Annales Geophysicae* **15**, 1340–1353.

Christopoulos, S., Koutitas, C., Soukissian, T. and Perivoliotis, L. (2000) Preliminary numerical results of the DAUT forecasting wave model in the context of the POSEIDON project. In *Proceedings of the Sixth Hellenic Symposium on Oceanography and Fisheries, Chios, 23–26 May 2000*, pp. 407–411. ISBN 960-85952-8-2.

Cressman, G. (1959) An operational objective analysis system. *Monthly Weather Review* **87**, 367–374.

Flemming, N. C. (1995) Making the case for GOOS. *Sea Technology, Special Feature*, pp. 44–49.

Hansen, S. E. and Stel, J. H. (1997) SEAWATCH. Performance and future. In *Operational Oceanography. The Challenges for European Co-operation*, ed. J. H. Stel. Elsevier Oceanography Series, 62, Elsevier, Amsterdam.

Horton, C., Clifford, M., Schmitz, J. and Kantha, L. H. (1997) A real time oceanographic nowcast/forecast system for the Mediterranean Sea. *Journal of Geophysical Research* **102**(C11), 25, 125–156.

IOC, (1998) The GOOS 1998, IOC, Paris, ISBN0-904175-39-1, 168 p.

Janjic, Z. I. (1994) The step-mountain eta coordinate model: further developments of the convection, viscous sublayer and turbulence closure schemes. *Monthly Weather Review* **122**, 927–945.

Kallos, G., Nickovic, S., Papadopoulos, A., Jovic, D., Kakaliagou, O., Misirlis, N., Boukas, L., Mimikou, N., Sakellaridis, G., Papageorgiou, J., Anadranistakis, E. and Manousakis, M. (1997) The regional weather forecasting system Skiron: An overview. In *Proceedings of the Symposium on Regional Weather Prediction on Parallel Computer Environments*, pp. 109–122. 15–17 October 1997, Athens, Greece.

Lascaratos, A. and Nittis, K. (1998) A high resolution 3-D numerical study of intermediate water formation in the Levantine Sea. *Journal of Geophysical Research* **13**(C9), 18497–18511.

McPhaden, M. J. (1995) The Tropical Atmosphere Ocean Array is completed. *Bulletin of the American Meteorological Society* **76**(5), 739–741.

Mellor, G. L. and Yamada, T. (1982) Development of a turbulence closure model for geophysical fluid problems. *Review of Geophysical Space Physics* **20**, 851–875.

Mesinger, F., Janjic, Z. I., Nickovic, S., Gavrilov, D. and Deaven, D. G. (1988) The step-mountain coordinate: model description and performance for cases of Alpine lee cyclogenesis and for a case of an Appalachian redevelopment. *Monthly Weather Review* **116**, 1493–1518.

Owens, W. B. and Millard, R. C. (1985) A new algorithm for CTD Oxygen Calibration. *Journal of Physical Oceanography* **15**(5), 621–631.

Nittis, K. and Lascaratos, A. (1998) Diagnostic and prognostic numerical studies of LIW formation. *Journal of Marine Systems* **18**, 179–195.

Pinardi, N. and Flemming, N. C. (1998) The Mediterranean Forecasting System Science Plan. EuroGOOS Publications No. 11, Southampton Oceanography Centre, Southampton, ISBN 0-904175-35-9.
Soukissian, T., Chronis, G. and Nittis, K. (1999) POSEIDON: operational marine monitoring system for Greek seas. *Sea Technology* **40**(7), 31–37.
Sverdrup, H. U. (1953) On conditions for the vernal blooming of phytoplankton. *Journal of Cons. Perm. Int. Exp. Mer*. **18**, 287–295.
Wilks, D. (1995) *Statistical Methods in the Atmospheric Sciences: An Introduction*. Academic Press, New York, 467 pp.
Woods, J. D., Dahlin, H., Droppert, L., Glass, M., Valerga, S. and Flemming, N. C. (1996) The Plan for EuroGOOS, EuroGOOS publication No. 3, Southampton Oceanography Centre, Southampton, ISBN 0-904175-26-X.
Yentsch, C. S. and Menzel, D. W. (1963) A method for the determination of phytoplankton chlorophyll and phaeophytin by fluorescence. *Deep-Sea Research* **10**, 221–231.
Zavatarelli, M. and Mellor, G. L. (1995) A numerical study of the Mediterranean Sea circulation, *Journal of Physical Oceanography* **25**(6), Part II, 1384–1414.
Zavaterelli, M. and Pinardi, N. (1995) The Adriatic Sea general circulation: modelling with the Princeton Ocean Model, *Annales Geophysicae* **13**(suppl. 2), C251.